Accepted: 16 December 2020

Genomic integrity and mitochondrial metabolism defects in Warsaw syndrome cells: a comparison with Fanconi anemia

Roberta Bottega[1] | Silvia Ravera[2] | Luisa M. R. Napolitano[3] | Viviana Chiappetta[4] | Nicoletta Zini[5,6] | Barbara Crescenzi[7] | Silvia Arniani[7] | Michela Faleschini[1] | Giuseppe Cortone[3,8] | Flavio Faletra[1] | Barbara Medagli[3,9] | Fabio Sirchia[1] | Martina Moretti[7] | Job de Lange[10] | Enrico Cappelli[11] | Cristina Mecucci[7] | Silvia Onesti[3] | Francesca M. Pisani[4] | Anna Savoia[1,12]

[1]Institute for Maternal and Child Health—IRCCS Burlo Garofolo, Trieste, Italy

[2]Department of Experimental Medicine, University of Genova, Genova, Italy

[3]Structural Biology Laboratory, Elettra-Sincrotrone Trieste, Trieste, Italy

[4]Istituto di Biochimica e Biologia Cellulare (IBBC), Consiglio Nazionale delle Ricerche (CNR), Naples, Italy

[5]CNR—National Research Council of Italy, Institute of Molecular Genetics "Luigi Luca Cavalli-Sforza"—Unit of Bologna, Bologna, Italy

[6]IRCCS Istituto Ortopedico Rizzoli, Bologna, Italy

[7]Sezione di Ematologia ed Immunologia Clinica, Centro Ricerche Emato-Oncologiche, University of Perugia, Perugia, Italy

[8]International School for Advanced Studies (SISSA), Trieste, Italy

[9]Department of Chemical and Pharmaceutical Sciences, University of Trieste, Trieste, Italy

[10]Amsterdam UMC, Clinical Genetics, Section Oncogenetics, Cancer Center Amsterdam, Amsterdam, The Netherlands

[11]UO Ematologia, IRCCS Istituto Giannina Gaslini, Genova, Italy, Genova, Italy

[12]Department of Medical Sciences, University of Trieste, Trieste, Italy

Correspondence
Anna Savoia, IRCCS Burlo Garofolo—Department of Medical Sciences, University of Trieste, via Dell'Istria, 65/1-I-34137 Trieste, Italy.
Email: anna.savoia@burlo.trieste.it

Disclosures: Roberta Bottega and Silvia Ravera should be considered joint firstauthor.

Funding information
Regione Campania, Grant/Award Number: POR-FESR 2014-2020 Progetto SATIN; European Union's H2020 MSCA-ETN 2019, Grant/Award Number: "AntiHelix", Grant Agreement N° 859853; IRCCS Burlo Garofolo, Grant/Award Number: Ricerca corrente 03/2018; AIRC 5x1000, Grant/Award Number: Mynerva project; Consorzio CNCCS:, Grant/Award Number: "Progetto B - Ricerca nuovi farmaci per malattie rare trascurate e della povertà"; Associazione Italiana per la

Abstract

Warsaw breakage syndrome (WABS), is caused by biallelic mutations of *DDX11*, a gene coding a DNA helicase. We have recently reported two affected sisters, compound heterozygous for a missense (p.Leu836Pro) and a frameshift (p.Lys303Glufs*22) variant. By investigating the pathogenic mechanism, we demonstrate the inability of the DDX11 p.Leu836Pro mutant to unwind forked DNA substrates, while retaining DNA binding activity. We observed the accumulation of patient-derived cells at the G2/M phase and increased chromosomal fragmentation after mitomycin C treatment. The phenotype partially overlaps with features of the Fanconi anemia cells, which shows not only genomic instability but also defective mitochondria. This prompted us to examine mitochondrial functionality in WABS cells and revealed an altered aerobic metabolism. This opens the door to the further elucidation of the molecular and cellular basis of an impaired mitochondrial phenotype and sheds light on this fundamental process in cell physiology and the pathogenesis of these diseases.

KEYWORDS
Fanconi anemia, genomic integrity, mitochondrial defects, oxidative stress, OXOPHOS, Warsaw syndrome

1 | INTRODUCTION

Warsaw breakage syndrome (WABS; MIM #613398, also called "Warsaw breakage syndrome") is an autosomal recessive disease characterized by prenatal and postnatal growth delay with microcephaly and other features, including intellectual disability, hearing loss, skin pigmentation abnormalities, and other congenital malformations (Alkhunaizi et al., 2018; Pisani, 2019; van der Lelij, Chrzanowska, et al., 2010). WABS is caused by mutations of *DDX11*, the gene that encodes an adenosine triphosphate (ATP)-dependent DNA helicase with a 5′–3′ DNA unwinding directionality. DDX11 (also known as ChlR1, Figure 1a) belongs to the super-family 2 DNA helicase group, and is characterized by the presence of an iron-sulfur (Fe-S) cluster (Bharti et al., 2014; Pisani et al., 2018). WABS cells display sister chromatid cohesion defects with a typical railroad chromosome structure, which classifies WABS as a cohesinopathy along with Cornelia de Lange (MIM #122470, for the most mutated gene, *NIPBL*) and Roberts (MIM #268300, *ESCO2*) syndromes (van der Lelij, Chrzanowska, et al., 2010). An increase of spontaneous and mitomycin C (MMC)-induced chromosomal breakages has also been reported, although not all WABS patient-derived cells may display enhanced chromosomal damage in response to clastogenic agents (as MMC or diepoxibutane [DEB]; van der Lelij, Chrzanowska, et al., 2010).

In addition to DDX11, the Fe-S DNA helicase group includes FANCJ, xeroderma pigmentosum complementation group D (XPD), and RTEL1, whose loss-of-function mutations are associated with rare genetic syndromes, such as Fanconi anemia complementation group J (FA-J; MIM #609054), XPD (MIM #278730), and dyskeratosis congenita (MIM #608833), respectively (Brosh, 2013). In particular, Fanconi anemia (FA) is characterized by congenital malformations, early-onset bone marrow failure, and cancer predisposition (Auerbach, 2009). In addition to *FANCJ*, other 21 genes are responsible for this disease with *FANCA* being the most frequently mutated gene (60–80%, FA-A; MIM #227650). The FA proteins play a role in a pathway controlling genomic stability, which is highlighted by the sensitivity of the FA cells to cross-linking agents (MMC and DEB) (Wang, 2007). Moreover, FA cells display altered mitochondria, characterized by swollen matrix with *cristae* less defined (Ravera et al., 2013) and impairment of oxidative phosphorylation (OXPHOS), which determines cellular energy unbalance, increment of the oxidative stress production, and switch from aerobic to anaerobic metabolism (Cappelli et al., 2017; Kumari et al., 2014).

To our knowledge, only 23 individuals with WABS have been reported in the literature (Alkhunaizi et al., 2018; Bailey et al., 2015; Bottega et al., 2019; Capo-Chichi et al., 2013; Eppley et al., 2017; Rabin et al., 2019; van der Lelij, Chrzanowska, et al., 2010; van Schie et al., 2020). They include two siblings we have recently described as compound heterozygous for the c.2507T>C (p.Leu836Pro) and c.907_920del (p.Lys303Glufs*22) mutations of *DDX11*, whose pathogenicity was established by bioinformatics studies and analysis of protein expression level in patient cells (Bottega et al., 2019). In this paper, we further explore the pathogenic effect of the p.Leu836Pro mutation, showing that the mutant protein is mainly located in the cytoplasm and unable to unwind DNA, while it retains the ability to bind to nucleic acid molecules. Consistently with a DDX11 role in maintaining genome stability, the cells of these two affected individuals are sensitive to MMC and show chromatid cohesion defects. Finally, we report for the first time that, despite their structural and morphological integrity, their mitochondria are functionally defective, suggesting that—as observed in FA (Bottega et al., 2018; Cappelli et al., 2017)—alterations of the mitochondrial activity may also contribute to WABS molecular pathogenesis.

2 | MATERIALS AND METHODS

2.1 | Cell culture and chromosome instability tests

Patient's and wild-type (WT) lymphoblast cell lines (LFB) were generated from primary lymphocytes isolated from peripheral blood as previously described (Bottega et al., 2019). Cells were grown at 37°C in RPMI1640 medium supplemented with 10% (v:v) foetal bovine serum and 1% (v/v) L-glutamine and penicillin/streptomycin (Gibco).

Both DEB and MMC were added after 24 h of culture. After 48 h of cross-linking treatment, cells in metaphases were blocked using colcemid for two hours. Slides were stained by Wright solution. In the DEB test, 16 normal controls were analysed evaluating break and gap events in 50 metaphases from the 1 μM DEB culture, and in 100 methaphases from no DEB culture. In the MMC test, break and gap events were analysed in 100 metaphases from both no MMC and 30 ng/ml MMC cultures derived from eight normal controls. The normal range of chromosome breakage was calculated according to our laboratory diagnostic standard. Chromatid gaps and breaks and interchanges (triradial/quadriradial figures) were expressed as number of events per cell.

2.2 | Protein expression

Protein whole and fractionated cell extracts were prepared from patients' lymphoblastoid cell lines (LCLs) as previously described (Bottega et al., 2018). Briefly, M-PER™ Mammalian Protein Extraction Reagent and NE-PER™ Nuclear and Cytoplasmic Extraction Reagents (Thermo Fisher Scientific), respectively, were used. Primary antibodies used were anti-DDX11 (sc-271711; Santa Cruz), anti-Sp1 (sc-17824; Santa Cruz), and anti-Hsp90 (sc-13119; Santa Cruz,). Immunoreactivity was visualized using the Enhanced Chemiluminescent SuperSignal™ West Femto Maximum Sensitivity Substrate (Pierce). The protein amount in each subcellular fraction was calculated by densitometric analysis and normalized with respect to the total amount of DDX11.

2.3 | Analysis of metaphase chromosome spreads with CREST immunofluorescence

Immunofluorescence analysis of metaphase chromosome spreads using the human CREST antibody was carried out as previously described with minor modifications (Cortone et al., 2018). LCLs derived from a healthy individual (WT) and from the WABS patients were seeded at a density of 1×10^5 cells/ml in RPMI1640 medium

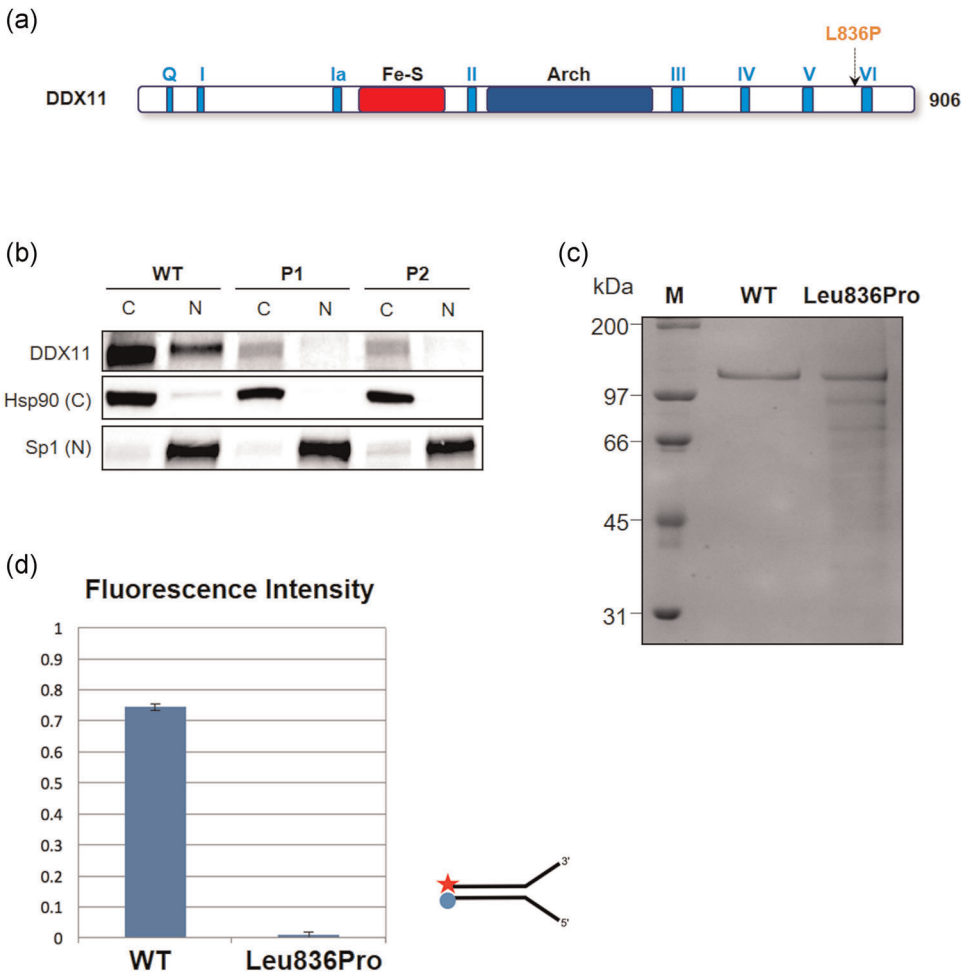

FIGURE 1 Protein expression, cellular localization, and biochemical analysis of DDX11 L836P mutant. (a) A schematic diagram of the architecture of the human DDX11 helicase: in red the Fe-S domain; in the dark blue the characteristic ARCH domain; in light blue the helicase motifs; the position of the mutation Leu836 is shown. (b) Western blot analysis of cytoplasmic (C) and nuclear (N) fractionated cellular lysate of patient-derived LCLs showing that a smaller amount (14.1% in P1 and 8.5% in P2) of the endogenous Leu863Pro protein compared to WT (37%) is located into the nucleus. Sp1 and Hsp90 are nuclear and cytoplasmic protein controls, respectively. (c) Coomassie-blue stained SDS-PAGE analysis of the recombinant WT and Leu836Pro mutant forms of DDX11, expressed and purified from baculovirus-infected insect cells; the predicted molecular weight is approximately 110 kDa; M: molecular weight protein standards. (d) Helicase activity of DDX11-WT and Leu836Pro mutant on a DNA fork, using a FRET-based assay: the fluorescence intensity reported is relative to the intensity of the boiled substrate. On the right-hand side, a schematic diagram of the DNA fork substrate: the red star represents the 6FAM fluorophore, the blue circle the BHQ1 quencher. While DDX11-WT is an active helicase, the p.Leu836Pro mutant shows no helicase activity. The assays have been carried out in triplicates. 6FAM, 6-carboxyfluorescein; FRET, fluorescence resonance energy transfer; LCL, lymphoblastoid cell line; SDS-PAGE, sodium dodecyl sulfate polyacrylamide gel electrophoresis; WT, wild type

supplemented with 10% (v:v) foetal bovine serum (Gibco), 1% (v/v) L-glutamine and penicillin/streptomycin (GIBCO). After 24 h, colchicin was added at 22.5 μg/ml and cells were incubated overnight (16 h) before being spun down (10 min at 100*g*). Cell pellets were resuspended in 0.5 ml of fresh medium, followed by drop-by-drop addition of a solution of KCl at 55 mM (3 ml) preheated at 37°C. Then, an additional aliquot (7 ml) of the same KCl solution was added into each sample all at once following by incubation at 37°C for 15 min. Then, samples were centrifuged at 100*g* for 10 min and resuspended in a solution of KCl at 55 mM at a density of about 2×10^5 cells/ml. Aliquots of 0.25 and 0.5 ml of each sample were spun onto microscope slides with a Shandon Cytospin centrifuge (Thermo Fisher Scientific) at 1000*g* per 4 min at the maximal acceleration. For detection of centromeres with the CREST antibody (donated by Florence Larminat, Toulouse, France) cells on the slides were treated exactly as previously described (Cortone et al., 2018). After 4′,6-diamidino-2-phenylindole counterstaining slides were analysed with a ×100 objective on a Nikon A1 confocal microscope using a NIS-Elements imaging software. Cohesion defects were expressed as % of cells with railroads and/or premature chromatid separation.

2.4 | Plasmids

Human DDX11 complementary DNA (cDNA) was cloned into pFB_ZB vector (a kind gift from the Structural Genomic Consortium, Oxford) or a pcDNA™3.1(+) Mammalian Expression Vector (Invitrogen). The L836P mutation was generated with the QuikChange site-directed mutagenesis kit (Stratagene). All plasmids were sequenced to verify that no desired mutations were introduced during polymerase chain reaction and cloning.

2.5 | Recombinant protein expression and purification

Recombinant baculovirus was generated by transfecting the pFB_ZB-hDDX11 construct into Sf9 cells using the polyethyleneimine method (Longo et al., 2013). High Five insect cells were infected with the virus for 72 h at 27°C. The pellet was resuspended in buffer A (25 mM Tris-HCl pH 7.4, 500 mM NaCl, 2 mM imidazole, 5% glycerol, 10 mM $MgCl_2$) in the presence of protease inhibitors (Roche). Cell disruption was carried out using French Press and the supernatant purified on a Ni-NTA Agarose resin (Qiagen), followed by Heparin-affinity chromatography (GE Healthcare).

2.6 | Helicase assays

DNA oligonucleotides used as substrates (Sigma-Aldrich) are listed in Table S2. DNA annealing was performed in 10 mM Tris-HCl pH 7.5, 50 mM NaCl, 1 mM EDTA pH 8.0. Strands D1:D2 (for the helicase assays) and D1:D3 (for the DNA binding assay) were annealed at a 1:3 molar ratio by heating at 95°C for 5 min, followed by slow cooling to room temperature.

FRET-based helicase assays (Tani et al., 2010) were performed on an Infinite F200 PRO Tecan instrument at 37°C in 30 μl reactions containing 90 nM hDDX11 proteins and 40 nM of dsDNA fork (D1:D2) in 5 mM HEPES-NaOH pH 7.5, 25 mM potassium acetate, 1 mM magnesium acetate, 10 mM NaCl, 1 mM dithiothreitol, in the presence of 500 nM Capture Strand (Cap1, Table S2). The reaction was started by adding ATP to a final concentration of 5 mM, and the increase in fluorescence monitored for 30 min. The fluorescence corresponding to 100% unwinding was evaluated by incubation at 95°C, and measurement in the absence of the protein subtracted from the data. The assays were carried out in triplicate.

2.7 | Electrophoretic mobility shift assays (EMSAs)

Nucleic acid-binding experiments were performed in the same buffer used for the helicase assays in presence of either 5 mM ATP or ATPγS, with 10 nM substrate (D1:D3) and increasing concentrations (0–400 nM) of the purified proteins in 30 μl of reaction volume, incubated at room temperature for 30 min in a dark environment. The reaction mixture was then loaded onto a 6% nondenaturing polyacrylamide gel and run in TBE buffer. Fluorescent labeled substrates were detected by the ImageQuant system (GE Healthcare).

2.8 | Evaluation of the ATP/AMP ratio

The amounts of ATP and AMP were quantified spectrophotometrically, following the NADP reduction or NADH oxidation at 340 nm, respectively (Columbaro et al., 2014). For each assay, 20 μg of total protein were employed and the NADPH and NADH molar extinction coefficient was considered 6.22 $mM^{-1} \cdot cm^{-1}$ at 340 nm.

2.9 | Evaluation of oxygen consumption rate and ATP synthesis as marker of OXPHOS function

Oxygen consumption rate was measured at 37°C in a closed chamber, using an amperometric electrode (Unisense-Microrespiration, Unisense A/S) (Columbaro et al., 2014). For each experiment, 200,000 cells were used. Cells were permeabilized with 0.03 mg/ml digitonin for 1 min, centrifuged for 9 min at 5000*g* and resuspended in a medium containing: 120 mM NaCl, 2 mM $MgCl_2$, 1 mM KH_2PO_4, 50 mM Tris-HCl, pH 7.4, and 25 mg/ml ampicillin. A total of 10 mM pyruvate and 5 mM malate or 20 mM succinate were added to stimulate the pathways composed of Complexes I, III, and IV or Complexes II, III, and IV, respectively.

ATP synthesis through F_o-F_1 ATP synthase was evaluated on 200,000 cells. Samples were incubated for 10 min at 37°C in 100 mM Tris/HCl (pH 7.4), 100 mM KCl, 1 mM EGTA, 2.5 mM EDTA, 5 mM $MgCl_2$, 0.2 mM di (adenosine-5′) penta-phosphate, 0.6 mM ouabain, ampicillin (25 μg/ml), 5 mM KH_2PO_4, and 10 mM pyruvate + 5 mM

malate or 20 mM succinate. ATP synthesis was then induced by adding 0.1 mM ADP. The reaction was monitored for two minutes, every 30 s, in a luminometer (GloMax® 20/20n Luminometer; Promega), by the luciferin/luciferase chemiluminescent method, with ATP standard solutions between 10^{-8} and 10^{-5} M (luciferin/luciferase ATP bioluminescence assay kit CLSII; Roche; Ravera et al., 2016).

2.10 | Lactate dehydrogenase (LDH) assay

LDH (EC: 1.1.1.27) activity was assayed on 20 μg of total protein, following NADH oxidation at 340 nm (Ravera et al., 2016).

2.11 | Assay of the respiratory complexes activity

The activity of the four electron transport chain complexes was assayed on 50 μg of total protein (Bartolucci et al., 2015).

Complex I (NADH-ubiquinone oxidoreductase) and Complex II (succinic dehydrogenase) activities were assayed following the reduction of ferricyanide at 420 nm. For both assays, ferricyanide molar extinction coefficient was considered 1 $mM^{-1}{\cdot}cm^{-1}$, at 420 nm.

To measure Complex III (Cyt c reductase) and Complex IV (Cyt c oxidase) activities, the reduction or the oxidation of Cyt c was followed at 550 nm, respectively. For both assays, Cyt c molar extinction coefficient was considered 19.1 $mM^{-1}{\cdot}cm^{-1}$, at 550 nm.

2.12 | Electron microscopy

LCL pellets were fixed with 2.5% glutaraldehyde in 0.1 M cacodylate buffer pH 7.4 for 2 h at room temperature, postfixed with 1% OsO_4 in cacodylate buffer for 1 h, dehydrated in an ethanol series, and embedded in Epon resin. Ultrathin sections stained with uranyl-acetate and lead citrate were observed with a Jem-1011 transmission electron microscope (Jeol).

3 | RESULTS

3.1 | Pathogenicity of p.Leu836Pro: Unstable and mainly cytoplasmic mutant that binds DNA but is defective in DNA unwinding

To determine the expression level and the cellular sublocalization of DDX11, we carried out western blot analysis of fractionated cell extract of LCLs established from the two affects siblings (P1 and P2). According to ACMG guidelines (Richards et al., 2015), the frameshift mutation was classified as pathogenic, which was confirmed by absence of any product of the expected size (35 kDa) in patients' cells (data not shown). Therefore, the protein recognized by the specific antibody is the p.Leu836Pro mutant form (classified as "Likely pathogenetic" by ACMG guidelines) of DDX11 codified by the other allele, whose expression level is significantly reduced (20%) compared to the wild-type protein (110 kDa) (Figure 1b). In addition to its lower expression level, the Leu836Pro variant is mainly localized in the cytoplasm (85.6% and 91.5% in P1 and P2, respectively), with only a small fraction (14.4% and 8.5% in P1 and P2, respectively) detectable in the nucleus, whereas approximately 37% of the WT protein has a nuclear localization (Figure 1b). The nuclear localization signal (residues, 295–312) is located in the Fe-S domain of DDX11 and is not adjacent to the predicted location of Leu836, suggesting that the disease-causing mutation is likely to affect the nuclear localization of DDX11 through its effect on protein folding and stability.

DDX11 is an helicase essential for the correct assembly of cohesin onto DNA (Cortone et al., 2018; Parish et al., 2006; Pisani et al., 2018). To confirm the pathogenic significance of the missense p.Leu836Pro variant, we thus analyzed the helicase activity and the DNA binding ability of the recombinant Leu836Pro mutant form of DDX11. We expressed the recombinant human WT and mutant DDX11 in baculovirus-infected insect cells. Both proteins were purified to near homogeneity and in relatively large amount, as highlighted by the appearance of single bands of 110 kDa after electrophoresis on Coomassie-stained sodium dodecyl sulfate polyacrylamide gel (Figure 1c). However, the presence of lower molecular weight products suggests that the mutant protein is more prone to proteolysis likely due to instability and partial misfolding.

To evaluate the DNA unwinding activity of mutant DDX11, we used a fluorescence-based helicase assay; to account for the presence of proteolysis fragments in the Leu836Pro mutant and provide a meaningful comparison, protein concentration was estimated for both the wild-type and the mutant based on the relative intensities of the 110 kDa bands, corresponding to the full length proteins, as shown in Figure 1c. The biochemical analysis showed that the WT recombinant DDX11 efficiently unwound DNA, whereas the Leu836Pro mutant had no helicase activity (Figure 1d).

A three-dimensional model of DDX11 (Bottega et al., 2019) suggests that the mutation is located at the interface between the helicase and the ARCH domains, and is close to the putative DNA binding path. To verify whether the helicase defect was due to impairment of the ability of the DDX11 mutant to bind nucleic acids, we tested the DNA-binding properties in EMSA, using the same DNA fork as a ligand, in presence of ATP and ATPγS. The mutant does bind nucleic acid, and the binding is stimulated by the presence of nucleotides, but at lower protein concentrations, has a slight affinity compared to the WT protein (Figure S1). Overall, these results seem to suggest that the Leu836Pro mutation maintains a 3D fold that is still able to bind nucleic acid and to interact similarly with ATP and ATPγS, but most likely disrupts the conformational changes required for unwinding.

3.2 | Features of chromosomal instability: Cohesion defects, G2/M arrest, and drug-induced chromosomal breakages

As DDX11 is essential for the correct assembly of cohesin onto DNA (Pisani et al., 2018), WABS cells are characterized by spontaneous

chromosomal cohesion defects (Alkhunaizi et al., 2018). To determine whether the DDX11 Leu836Pro mutation is associated with chromosomal cohesion defects, we examined the centromeric cohesion phenotype in metaphase chromosome spreads from LCLs of the two WABS patients (Figure 2a). Consistently, cells of our patients showed railroad chromosomes due to premature centromere division (PCD) or even a total premature centromere separation (PCS; van der Lelij, Chrzanowska, et al., 2010). In particular, we found that the percentage of chromosomes with loosened or separated centromeric constrictions is significantly higher in P1 (71%) and P2 (85%) cells than in control samples (35%) (Figure 2b). Moreover, the fraction of LCLs giving rise to metaphase chromosome spreads with PCS was remarkably increased in the two patients (17% in P1 and 28% in P2) compared to the healthy control (7%).

Regarding other chromosomal features of WABS, the pathognomonic significance of response to crosslinking agent is controversial, as the sensitivity to MMC and/or DEB varies among patients (Alkhunaizi et al., 2018). In particular, data from literature reported that cells from one affected individual showed increased chromosomal breakage when exposed to MMC, but not to DEB (Rabin et al., 2019), whereas no effect on chromosomal instability was detected in cells of two other patients after treatment with these two genotoxic agents (Alkhunaizi et al., 2018). For this reason, we analyzed the cell cycle to test the sensitivity of the P1 and P2, as well FA (FANCA−/−), patient-derived cell lines to cross-linking agents (melphalan—a nitrogen mustard alkylating agent—and MMC at two different concentrations). These analyses revealed that while FA cells are hypersensitive to melphalan, WABS cells are not (Figure 2c). Instead, they show significant ($p > .01$) increment of cells in G2/M phase after treatment with MMC. The arrest is similar but less extensive as that observed in FA cells ($p < .001$). Finally, we tested the response to DEB and MMC. Whereas MMC leads to an increase of chromosome aberrations, DEB has apparently no effect on chromosomal stability as the number of event/cells remain in the normal range (Table S1 and Figure S2). The percentage of cells with PCS was significantly higher (from 1–5% to 22.5–23.5%) after exposure to MMC, further confirming the sensitivity of the cell lines from our WABS patients to this cross-linking agent.

3.3 | Mitochondrial phenotype: Defective OXPHOS metabolism

Considering that WABS and FA display partly overlapping features in terms of genomic instability and FA cells show alterations of the mitochondrial morphology and function (Bottega et al., 2018; Capanni et al., 2013; Cappelli et al., 2017; Ravera et al., 2013), we investigated the structure and metabolism of these organelles in P1 and P2 cells. In contrast to what was observed in FA (Capanni et al., 2013; Ravera et al., 2013), the electron microscopy analyses showed that WABS mitochondria have normal structure with parallel *cristae* and dense mitochondrial matrix, similar to the control samples (Figure S3). However, despite the normal mitochondrial morphology, biochemical analyses indicate that WABS cells are characterized by altered aerobic metabolism. In particular, the two LCLs established from our patients and an immortalized fibroblast cell line derived from the first diagnosed WABS patient (*VU1202-F*) (van der Lelij, Chrzanowska, et al., 2010) show marked reduction of oxygen consumption and ATP synthesis in the presence of pyruvate/malate, similarly to that observed in FA cells (Cappelli et al., 2017; Ravera et al., 2013); they also show OXPHOS dysfunction in the presence of succinate, which is not detected in FA cells (Figure 3a,b).

Since the alteration of OXPHOS activity in FA cells depends on impairment of the electron transport between Complexes I and III (Cappelli et al., 2013, 2017), we analysed the activity of the single respiratory complex. All the WABS cells showed a normal activity of Complexes I and II, as found in FA cells (Figure S4), partial impairment of electron transport between Complexes I and III, more evident in the WABS immortalized fibroblasts than in P1 and P2 lymphoblasts (Figure 3c), and marked decrease of Complex IV activity, which is not observed in FA cells (Figure 3d).

To determine whether WABS patient-derived cells activate an alternative biochemical pathway in response to the OXPHOS alteration, we evaluated LDH activity. As shown in Figure 3f, WABS lymphoblast cells, as well as WABS fibroblasts, show an increment of LDH activity compared to the control samples, more evident in lymphoblast cells, suggesting an increment of the anaerobic glycolytic flux probably as attempt to restore the ATP intracellular pool. Similarly, FA cells are characterized by an increased anaerobic glycolysis. However, this “adaption mechanism” appears unsuccessful, as indicated by the low ATP/AMP ratio compared to control samples (Figure 3e). In particular, the impairment of energy balance seems to depend on both decrement in ATP level and increment of AMP content (Figure S5). A similar reduction of ATP/AMP ratio is recapitulated in FA lymphoblast cells, as previously described (Cappelli et al., 2013, 2017).

4 | DISCUSSION

DDX11 is a helicase essential for the correct assembly of cohesin onto DNA (Cortone et al., 2018; Parish et al., 2006; Pisani et al., 2018). In vitro, DDX11 has been shown to unwind several nonduplex DNA structures, such as G-quadruplexes (Bharti et al., 2013; Wu et al., 2012) ensuring that processive replication is maintained and thereby avoiding genetic instability. The helicase activity of DDX11 is stimulated by the interaction with Timeless (Calì et al., 2016; Cortone et al., 2018; Leman et al., 2010) which has a key role in both the preservation of fork progression under perturbed conditions (Calì et al., 2016) and sister chromatid cohesion (Cortone et al., 2018). More recently Lerner et al. (2010) showed that Timeless is required to maintain processive replication of G4 DNA suggesting that the recruitment of DDX11 to the replisome could be stimulated by G4 detection by Timeless.

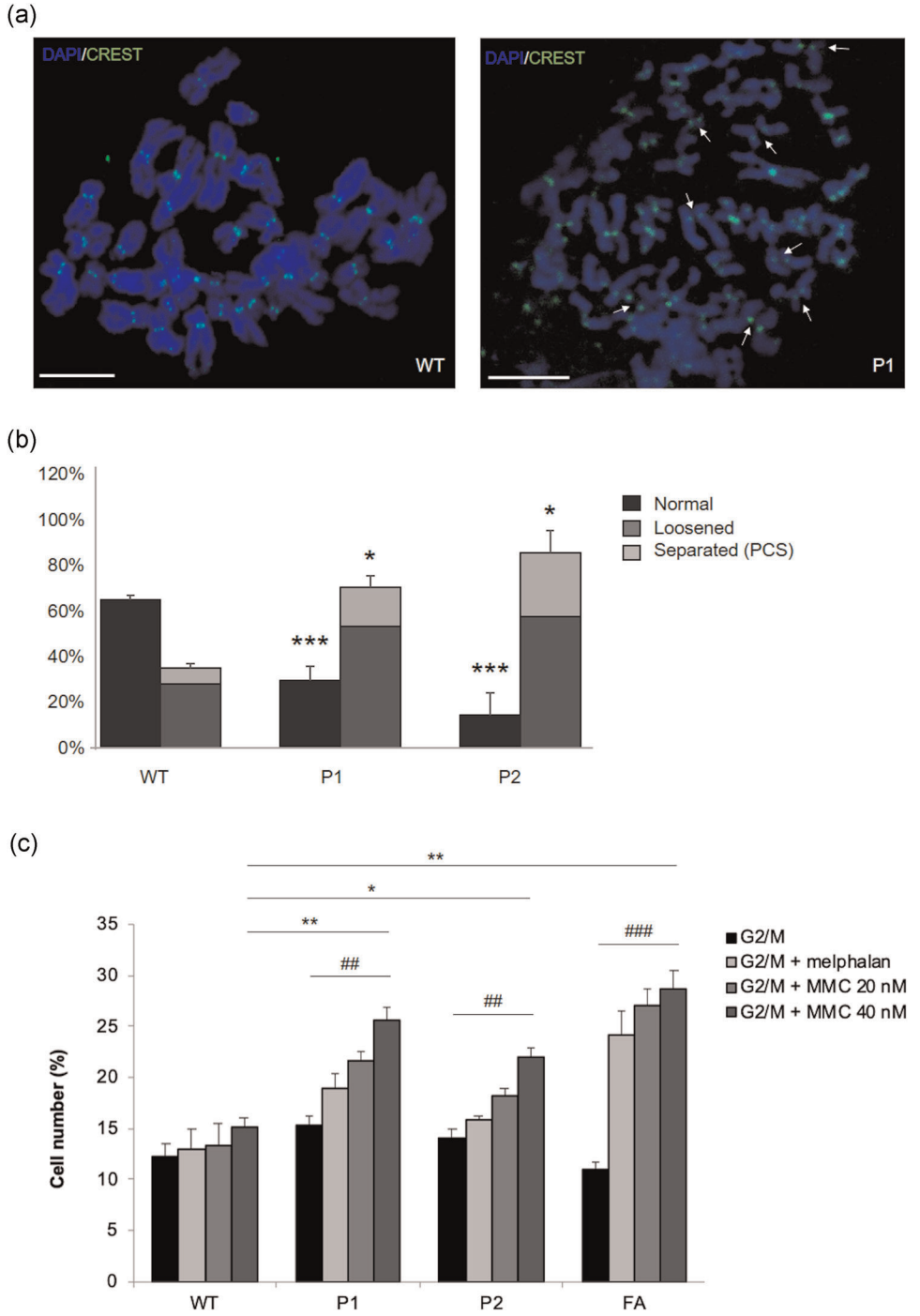

FIGURE 2 Analysis of cohesion defects and cell cycle analysis in LCLs from WABS patients. (a) Representative images of metaphase chromosome spreads prepared from LCL of a healthy individual (WT) and patient P1. Chromosomes were stained with DAPI (blue) and the human centromere/kinetochore marker CREST (green). Chromosomes with a loosened/separated centromere are indicated with arrows. Scale bar = 10 μm. (b) Plot showing frequency of the indicated chromosome configurations in spreads prepared from a healthy individual (WT) and patient-derived cell lines (P1 and P2). Spreads with at least four chromosomes with loosened/separated chromatids were classified as defective in cohesion. At least 40 spreads were examined for each LCL in two independent experiments. Values of $p < .01$ were calculated for WT versus P1 and P2 LCLs using Student's *t* test. (c) Percentage of LCLs from healthy individual (WT), WABS (P1 and P2), and FA (FANCA−/−) patients in G2/M phase after treatments with melphalan or MMC at two different concentrations (20 and 40 nM). *p* values were calculated for WT versus P1, P2 and FA LCLs treated with MMC 40 nM (*) or for untreated LCL versus the same LCL treated with MMC 40 nM (#) using that to Student's *t* test. Error bars represent *SE*. $^{*}p < .05$; ** and $^{\#\#}p < .01$; *** and $^{\#\#\#}p < .001$. DAPI, 4′,6-diamidino-2-phenylindole; LCL, lymphoblastoid cell line; WABS, Warsaw breakage syndrome; WT, wild type

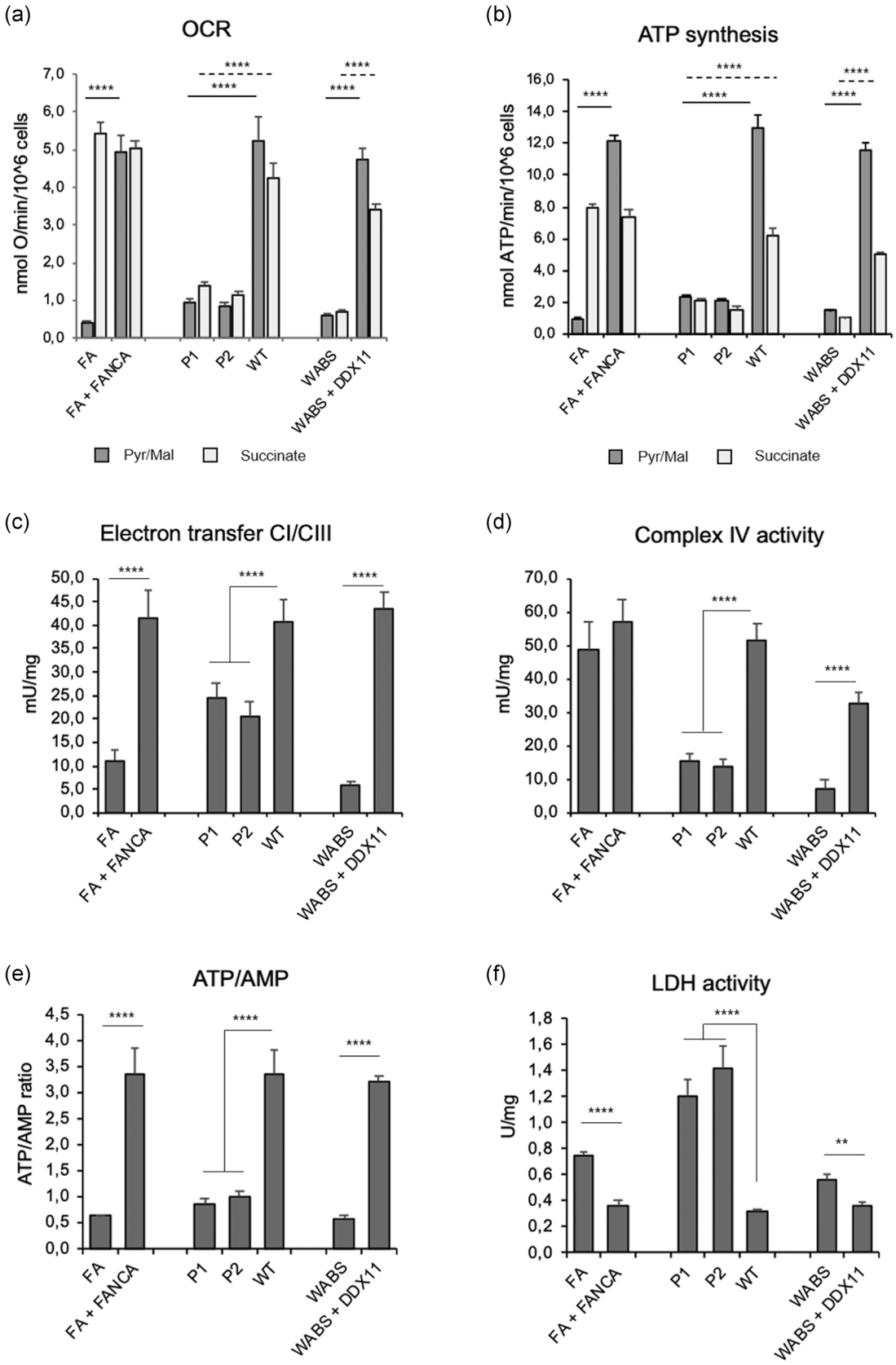

FIGURE 3 (See caption on next page)

Since its first report (van der Lelij, Chrzanowska, et al., 2010), WABS has been diagnosed in few families, including that we have recently described carrying bi-allelic mutations, c.2507T>C (p.Leu836Pro) and c.907_920del (p.Lys303Glufs*22), of the *DDX11* gene (Bottega et al., 2019). Whereas the first was clearly classified as pathogenetic, the missense one was considered to be deleterious based on its expression level that is significantly reduced in patients' cells, where it is almost totally detected in the cytoplasm. These data suggest that the p.Leu836Pro substitution is likely to affect not only stability but also the nuclear localization of DDX11.

The pathogenic significance of the DDX11 p.Leu836Pro change, was confirmed by in vitro biochemical assays showing that the p.Leu836Pro mutant lacks DNA helicase activity, though retaining a nucleotide-stimulated DNA binding capability.

Among the other mutant forms of DDX11 reported so far, only p.Arg263Gln (Capo-Chichi et al., 2013), which affects the Fe-S domain, Lys897del (van der Lelij, Chrzanowska, et al., 2010), which lacks a single lysine residue in the C-terminal end, and Cys705Tyr and Arg140Gln (van Schie et al., 2020), located in the N-terminal and C-terminal, respectively, were analyzed in vitro to elucidate their molecular defects. Whereas the Arg263Gln DDX11 recombinant protein appears to be stable and has been found to retain very low DNA melting and binding activity, the DDX11 Lys897del and Cys705Tyr forms are produced with a reduced yield and are unable to unwind and to bind to the forked duplex (Capo-Chichi et al., 2013; van der Lelij, Chrzanowska, et al., 2010; van Schie et al., 2020; Wu et al., 2012). The pathogenicity of mutant Arg140Gln DDX11 form remains unclear as it localize in the nucleus where it exert a normal helicase activity (van Schie et al., 2020).

Although limited to only a few mutations, the biochemical studies indicate that missense alleles of *DDX11* are likely to be loss-of-function mutations regardless of the stability and expression level of the mutant protein. Consistently, although partially stable and expressed in patients' cells, the Leu836Pro protein is hardly detectable in the nucleus and inactive as a helicase.

As mentioned above, DDX11 is essential for the correct assembly of cohesin onto DNA (Pisani et al., 2018) and consequently, WABS cells show spontaneous chromosomal cohesion defects, as observed in all the affected individuals reported so far (Alkhunaizi et al., 2018; van der Lelij, Chrzanowska, et al., 2010; van Schie et al., 2020). On the contrary, the pathognomonic significance of response to crosslinking agent is controversial, as the sensitivity to MMC and/or DEB varies among patients (Alkhunaizi et al., 2018).

Cells from our patients also showed the formation of railroad chromosomes due to PCD or even PCS while, cells' behavior in response to crosslinking agent was less uniform. In particular, cells from one affected individual showed increased chromosomal breakage when exposed to MMC, but not to DEB (Rabin et al., 2019), whereas no difference was detected in cells of two other patients after treatment with these two genotoxic agents. For this reason, we tested the effect of these two cross-linking agents and found that cells of P1 and P2 are sensitive to MMC but not to DEB. Consistent with genomic instability, the cells accumulated in G2/M in response to MMC, an increment that is almost similar to that obtained in FA cells. Using melphalan, a nitrogen mustard alkylating agent, the number of cells in the G2/M slightly increased but not as significantly as in FA.

Therefore, WABS and FA share some cellular features, such as hypersensitivity to MMC and its consequent arrest in G2/M, and cohesion abnormalities (van der Lelij, Oostra, et al., 2010). However, genomic stability is more preserved in WABS cells. In fact, while in WABS cells the chromosomal breakage is observable only after induction by a subset of chemicals, in FA cells it is spontaneous and can be aggravated by several genotoxic agents. On the contrary, the cohesion defect is more marked in WABS, as cells spontaneously—and not after induction like in FA (van der Lelij, Oostra, et al., 2010)—display premature centromere division or chromatid separation. The differential response to cross-linking agents strongly indicate that different, but partly overlapping, molecular pathways are altered in the two diseases.

Finally, considering that WABS and FA display overlapping features in terms of genomic instability, we investigated the integrity of mitochondria, which are morphologically and functionally altered in FA. In contrast to what observed in FA (Capanni et al., 2013; Ravera et al., 2013), WABS mitochondria have normal structure. However, our biochemical analyses indicate that WABS cells are characterized by altered aerobic metabolism, similar to that observed for FA cells (Cappelli et al., 2017; Ravera et al., 2013). The OXPHOS impairment in FA cells is evident after the activation with pyruvate/malate but not with succinate whereas in WABS cells OXPHOS is impaired with both substrates. Alteration of aerobic metabolism is due to respiratory complex dysfunction. In particular, WABS cells display a

FIGURE 3 Evaluation of energy metabolism. All analyses have been carried out on one FA and two WABS (P1 and P2) patient-derived LCLs, and one WABS immortalized fibroblast cell line (*VU1202-F*[1]) and the respective controls (FA + FANCA: FA LCL expressing WT FANCA cDNA; WT: wild type LCL; WABS + DDX11: WABS immortalized fibroblasts expressing wild type DDX11 cDNA). OCR (a) and ATP synthesis (b) were evaluated after the induction with pyruvate + malate (dark grey columns) or succinate (light grey columns), as markers of oxidative phosphorylation function. Electron transfer between Complexes I and III (c) and activity of Complex IV (d) were evaluated as markers of mitochondrial electron transport. ATP/AMP ratio (e) indicates the cellular energy status. (f) LDH activity was investigated as marker of lactate fermentation, the anaerobic counterpart of the glucose catabolism. Each graph is representative of four experiments carried out in each cell line and data are expressed as mean ± *SD*. *t* test indicates significant difference of $^{**}p < .01$ and $^{****}p < .0001$ between the mutated or patients' cells and the respective control. ATP, adenosine triphosphate; cDNA, complementary DNA; FA, Fanconi anemia; LCL, lymphoblastoid cell line; LDH, lactic dehydrogenase; OCR, oxygen consumption rate; WABS, Warsaw breakage syndrome

defect in the electron transport between Complexes I and III, and an impairment of Complex IV activity. Of note, although FA cells show the same electron transfer defect, the activity of Complex IV is in the normal range. Finally, both FA and WABS cells increase the anaerobic glycolytic flux, probably as attempt to restore the ATP intracellular pool. However, this strategy appears unsuccessful, as indicated by the low ATP/AMP ratio compared to control samples.

It is important to note that the decrease of ATP availability makes cells more fragile, since, in low energy *status*, managing the residual DNA repair capability and the oxidative stress associated with these diseases becomes more difficult.

The molecular mechanisms underlying the mitochondrial phenotype have not yet been elucidated either in WABS or in FA, even if the increased OXPHOS stress observed in FA has been known for a long time (Pagano et al., 2012). In FA, the mitochondrial phenotype could be explained by a role of the FA proteins not only in response to DNA damage but also in cytoplasmic processes, such as selective autophagy of mitochondria (Sumpter et al., 2016), a process that, when defective, results in accumulation of dysfunctional mitochondria. In WABS, mutations of DDX11 could lead to the altered expression of several genes, including those coding for ribosomal RNAs (rRNAs); it has been proposed that rRNA genes are positively regulated by DDX11, which specifically binds to their promoters in the nucleolus compartment (Sun et al., 2015). Decrease in rRNA synthesis could interfere with the correct expression of many proteins, including components of those respiratory complexes, whose functionality is affected WABS patient-derived cells (see Figure 3c,d). It is also possible that DDX11 could localize to the mitochondria and thus more directly affect mitochondrial metabolism. Although a bioinformatics analysis on the human DDX11 sequence does not reveal the obvious presence of a Mitochondrial Targeting Sequence (MTS), other mitochondrial proteins lack a canonical signal. Among those, it is noteworthy the XPD helicase, also belonging to the Fe-S helicase family; although it lacks a recognizable MTS, XPD was shown to be recruited to mitochondria, especially during oxidative stress, and is likely to be involved in the repair of mitochondrial DNA damage (Liu et al., 2015).

We present novel evidence that, similarly to FA, WABS is a chromosomal instability syndrome characterized by hypersensitivity to MMC and defective OXPHOS metabolism. The association of both DDX11 and FA mutations with defective mitochondrial activity is intriguing; further elucidation of the molecular and cellular basis of these associations will not only shed light on this fundamental process in cell physiology but will also provide the framework to fully understand these hereditary diseases.

ACKNOWLEDGEMENTS

This study was supported by IRCCS "Burlo Garofolo" (Ricerca Corrente 03/2018); AIRC Grants IG-14718, IG-20778, and IG-21974; the European Union's Horizon 2020 research and innovation program grant Agreement N° 859853 (MSCA-ETN 2019, "AntiHelix"); Consorzio CNCCS ("Progetto B—Ricerca di nuovi farmaci per malattie rare trascurate e della povertà"); Regione Campania (POR-FESR 2014-2020, "Progetto SATIN"); AIRC 5xmille, MYNERVA Project; the Cross-border Cooperation Programme Italy-Slovenia 2014–2020 by the European Regional Development Fund and national funds (TransGlioma). We thank the Elettra Protein Production Facility for the technical support. The authors thank the patients for their participation in this project and Prof. D. L. Gughi and Prof. F. Dede for the constructive discussions.

CONFLICT OF INTERESTS

The authors declare that there are no conflict of interests.

AUTHOR CONTRIBUTIONS

Roberta Bottega and Anna Savoia wrote the manuscript. Roberta Bottega, Anna Savoia, Nicoletta Zini, Cristina Mecucci, Silvia Onesti, and Francesca M. Pisani revised the manuscript critically for important intellectual content. Silvia Ravera, Luisa M. R. Napolitano, Viviana Chiappetta, Barbara Crescenzi, Silvia Arniani, Michela Faleschini, Giuseppe Cortone, Flavio Faletra, Flavio Faletra, Barbara Medagli, Fabio Sirchia, Martina Moretti, Job de Lange, and Enrico Cappelli made substantial contributions to conception design, acquisition, analysis, and interpretation of data. All authors give final approval of the version to be published and agree to be accountable for all technical and experimental aspects of the work.

DISCLOSURE

Roberta Bottega and Silvia Ravera should be considered joint first author.

DATA AVAILABILITY STATEMENT

The data that support the findings of this study are available from the corresponding author upon reasonable request.

ORCID

Roberta Bottega http://orcid.org/0000-0001-7431-7543
Silvia Ravera https://orcid.org/0000-0002-0803-1042
Nicoletta Zini https://orcid.org/0000-0002-4442-7079
Michela Faleschini https://orcid.org/0000-0001-5147-3164
Flavio Faletra https://orcid.org/0000-0003-1483-3612
Job de Lange https://orcid.org/0000-0002-9002-8829
Enrico Cappelli http://orcid.org/0000-0001-5910-9260
Cristina Mecucci https://orcid.org/0000-0002-1623-0148
Silvia Onesti https://orcid.org/0000-0002-0612-7948
Francesca M. Pisani https://orcid.org/0000-0002-4591-7571
Anna Savoia https://orcid.org/0000-0002-2407-2696

REFERENCES

Alkhunaizi, E., Shaheen, R., Bharti, S. K., Joseph-George, A. M., Chong, K., Abdel-Salam, G. M. H., Alowain, M., Blaser, S. I., Papsin, B. C., Butt, M., Hashem, M., Martin, N., Godoy, R., Brosh, R. M., Alkuraya, F. S., & Chitayat, D. (2018). Warsaw breakage syndrome: Further clinical and genetic delineation. *American Journal of Medical Genetics, Part A*, *176*(11), 2404–2418.

Auerbach, A. D. (2009). Fanconi anemia and its diagnosis. *Mutation Research/DNA Repair*, *668*(1–2), 4–10.

Bailey, C., Fryer, A. E., & Greenslade, M. (2015). Warsaw Breakage syndrome—A further report, emphasising cutaneous findings. *European Journal of Medical Genetics*, *58*(4), 235–237.

Bartolucci, M., Ravera, S., Garbarino, G., Ramoino, P., Ferrando, S., Calzia, D., Candiani, S., Morelli, A., & Panfoli, I. (2015). Functional expression of electron transport chain and FoF1-ATP synthase in optic nerve myelin sheath. *Neurochemical Research*, *40*(11), 2230–2241.

Bharti, S. K., Khan, I., Banerjee, T., Sommers, J. A., Wu, Y., & Brosh, R. M. (2014). Molecular functions and cellular roles of the ChlR1 (DDX11) helicase defective in the rare cohesinopathy Warsaw breakage syndrome. *Cellular and Molecular Life Science*, *71*(14), 2625–2639.

Bharti, S. K., Sommers, J. A., George, F., Kuper, J., Hamon, F., Shin-ya, K., Teulade-Fichou, M. P., Kisker, C., & Brosh, R. M. (2013). Specialization among iron-sulfur cluster helicases to resolve G-quadruplex DNA structures that threaten genomic stability. *Journal of Biological Chemistry*, *288*(39), 28217–29.

Bottega, R., Napolitano, L. M. R., Carbone, A., Cappelli, E., Corsolini, F., Onesti, S., Savoia, A., Gasparini, P., & Faletra, F. (2019). Two further patients with Warsaw breakage syndrome. Is a mild phenotype possible? *Molecular Genetics & Genomic Medicine*, *7*(5), e639.

Bottega, R., Nicchia, E., Cappelli, E., Ravera, S., De Rocco, D., Faleschini, M., Corsolini, F., Pierri, F., Calvillo, M., Russo, G., Casazza, G., Ramenghi, U., Farruggia, P., Dufour, C., & Savoia, A. (2018). Hypomorphic FANCA mutations correlate with mild mitochondrial and clinical phenotype in Fanconi anemia. *Haematologica*, *103*(3), 417–426.

Brosh, R. M. (2013). DNA helicases involved in DNA repair and their roles in cancer. *Nature Reviews Cancer*, *13*(8), 542–558.

Calì, F., Bharti., S. K., Di Perna, R., Brosh., R. M., Jr, & Pisani, F. M. (2016). Tim/Timeless, a member of the replication fork protection complex, operates with the Warsaw breakage syndrome DNA helicase DDX11 in the same fork recovery pathway. *Nucleic Acids Research*, *44*(2), 705–17.

Capanni, C., Bruschi, M., Columbaro, M., Cuccarolo, P., Ravera, S., Dufour, C., Candiano, G., Petretto, A., Degan, P., & Cappelli, E. (2013). Changes in vimentin, lamin A/C and mitofilin induce aberrant cell organization in fibroblasts from Fanconi anemia complementation group A (FA-A) patients. *Biochimie*, *95*(10), 1838–1847.

Capo-Chichi, J. M., Bharti, S. K., Sommers, J. A., Yammine, T., Chouery, E., Patry, L., Rouleau, G. A., Samuels, M. E., Hamdan, F. F., Michaud, J. L., Brosh, R. M., Jr., Mégarbane, A., & Kibar, Z. (2013). Identification and biochemical characterization of a novel mutation in DDX11 causing Warsaw breakage syndrome. *Human Mutation*, *34*(1), 103–107.

Cappelli, E., Cuccarolo, P., Stroppiana, G., Miano, M., Bottega, R., Cossu, V., Degan, P., & Ravera, S. (2017). Defects in mitochondrial energetic function compels Fanconi anaemia cells to glycolytic metabolism. *Biochimica et Biophysica Acta/General Subjects*, *1863*(6), 1214–1221.

Cappelli, E., Ravera, S., Vaccaro, D., Cuccarolo, P., Bartolucci, M., Panfoli, I., Dufour, C., & Degan, P. (2013). Mitochondrial respiratory complex I defects in Fanconi anemia. *Trends in Molecular Medicine*, *19*(9), 513–514.

Columbaro, M., Ravera, S., Capanni, C., Panfoli, I., Cuccarolo, P., Stroppiana, G., Degan, P., & Cappelli, E. (2014). Treatment of FANCA cells with resveratrol and N-acetylcysteine: A comparative study. *PLOS One*, *9*(7), e104857.

Cortone, G., Zheng, G., Pensieri, P., Chiappetta, V., Tatè, R., Malacaria, E., Pichierri, P., Yu, H., & Pisani, F. M. (2018). Interaction of the Warsaw breakage syndrome DNA helicase DDX11 with the replication fork-protection factor Timeless promotes sister chromatid cohesion. *PLOS Genetics*, *14*(10), e1007622.

Eppley, S., Hopkin, R. J., Mendelsohn, B., & Slavotinek, A. M. (2017). Clinical Report: Warsaw Breakage Syndrome with small radii and fibulae. *American Journal of Medical Genetics, Part A*, *173*(11), 3075–3081.

Kumari, U., Ya Jun, W., Huat Bay, B., & Lyakhovich, A. (2014). Evidence of mitochondrial dysfunction and impaired ROS detoxifying machinery in Fanconi anemia cells. *Oncogene*, *33*(2), 165–172.

van der Lelij, P., Chrzanowska, K. H., Godthelp, B. C., Rooimans, M. A., Oostra, A. B., Stumm, M., Zdzienicka, M. Z., Joenje, H., & de Winter, J. P. (2010). Warsaw breakage syndrome, a cohesinopathy associated with mutations in the XPD helicase family member DDX11/ChlR1. *American Journal of Human Genetics*, *86*(2), 262–266.

van der Lelij, P., Oostra, A. B., Rooimans, M. A., Joenje, H., & de Winter, J. P. (2010). Diagnostic overlap between fanconi anemia and the cohesinopathies: Roberts syndrome and Warsaw breakage syndrome. *Anemia*, *2010*, 565268.

Leman, A. R., Noguchi, C., Lee, C. Y., Noguchi, E. (2010). Human Timeless and Tipin stabilize replication forks and facilitate sister-chromatid cohesion. *Journal of Cell Science*, *123*(Pt 5), 660–70.

Lerner, L. K., Holzer, S., Kilkenny, M. L., Šviković, S., Murat, P., Schiavone, D., Eldridge, C. B., Bittleston, A., Maman, J. D., Branzei, D., Stott., K., Pellegrini., L., & Sale, J. E. (2020). Timeless couples G-quadruplex detection with processing by DDX11 helicase during DNA replication. *EMBO Journal*, *39*(18), e104185.

Liu, J., Fang, H., Chi, Z., Wu, Z., Wei, D., Mo, D., Niu, K., Balajee, A. S., Hei, T. K., Nie, L., & Zhao, Y. (2015). XPD localizes in mitochondria and protects the mitochondrial genome from oxidative DNA damage. *Nucleic Acids Research*, *43*(11), 5476–5488.

Longo, P. A., Kavran, J. M., Kim, M. S., & Leahy, D. J. (2013). Transient mammalian cell transfection with polyethylenimine (PEI). *Methods in Enzymology*, *529*, 227–240.

Pagano, G., Talamanca, A. A., Castello, G., Pallardó, F. V., Zatterale, A., & Degan, P. (2012). Oxidative stress in Fanconi anaemia: From cells and molecules towards prospects in clinical management. *Biological Chemistry*, *393*(1-2), 11–21.

Parish, J. L., Rosa, J., Wang, X., Lahti, J. M., Doxsey, S. J., & Androphy, E. J. (2006). The DNA helicase ChlR1 is required for sister chromatid cohesion in mammalian cells. *Journal of Cell Science*, *119*(Pt 23), 4857–4865.

Pisani, F. M. (2019). Spotlight on Warsaw breakage syndrome. *The Application of Clinical Genetics*, *12*, 239–248.

Pisani, F. M., Napolitano, E., Napolitano, L. M. R., & Onesti, S. (2018). Molecular and cellular functions of the Warsaw breakage syndrome DNA helicase DDX11. *Genes (Basel)*, *9*, 11.

Rabin, R., Hirsch, Y., Johansson, M. M., Ekstein, J., Zeevi, D. A., Keena, B., Zackai, E. H., & Pappas, J. (2019). Study of carrier frequency of Warsaw breakage syndrome in the Ashkenazi Jewish population and presentation of two cases. *American Journal of Medical Genetics, Part A*, *179*(10), 2144–2151.

Ravera, S., Dufour, C., Cesaro, S., Bottega, R., Faleschini, M., Cuccarolo, P., Corsolini, F., Usai, C., Columbaro, M., Cipolli, M., Savoia, A., Degan, P., & Cappelli, E. (2016). Evaluation of energy metabolism and calcium homeostasis in cells affected by Shwachman-Diamond syndrome. *Scientific Reports*, *6*, 25441.

Ravera, S., Vaccaro, D., Cuccarolo, P., Columbaro, M., Capanni, C., Bartolucci, M., Panfoli, I., Morelli, A., Dufour, C., Cappelli, E., & Degan, P. (2013). Mitochondrial respiratory chain Complex I defects in Fanconi anemia complementation group A. *Biochimie*, *95*(10), 1828–1837.

Richards, S., Aziz, N., Bale, S., Bick, D., Das, S., Gastier-Foster, J., Grody, W. W., Hegde, M., Lyon, E., Spector, E., Voelkerding, K., & Rehm, H. L. (2015). Standards and guidelines for the interpretation of sequence variants: A joint consensus recommendation of the American College of Medical Genetics and Genomics and the Association for Molecular Pathology. *Genetics in Medicine*, *17*(5), 405–424.

van Schie, J. J. M., Faramarz, A., Balk, J. A., Stewart, G. S., Cantelli, E., Oostra, A. B., Rooimans, M. A., Parish, J. L., de Almeida Estéves, C., Dumic, K., Barisic, I., Diderich, K. E. M., van Slegtenhorst, M. A., Mahtab, M., Pisani, F. M., te Riele, H., Ameziane, N., Wolthuis, R. M. F., & de Lange, J. (2020). Warsaw breakage syndrome associated DDX11 helicase resolves G-quadruplex structures to support sister chromatid cohesion. *Nature Communications, 11*(1), 4287.

Sumpter, R., Sirasanagandla, S., Fernández, Á. F., Wei, Y., Dong, X., Franco, L., Zou, Z., Marchal, C., Lee, M. Y., Clapp, D. W., Hanenberg, H., & Levine, B. (2016). Fanconi anemia proteins function in mitophagy and immunity. *Cell*, *165*(4), 867–881.

Sun, X., Chen, H., Deng, Z., Hu, B., Luo, H., Zeng, X., Han, L., Cai, G., & Ma, L. (2015). The Warsaw breakage syndrome-related protein DDX11 is required for ribosomal RNA synthesis and embryonic development. *Human Molecular Genetics*, *24*(17), 4901–4915.

Tani, H., Fujita, O., Furuta, A., Matsuda, Y., Miyata, R., Akimitsu, N., Tanaka, J., Tsuneda, S., Sekiguchi, Y., & Noda, N. (2010). Real-time monitoring of RNA helicase activity using fluorescence resonance energy transfer in vitro. *Biochemical and Biophysical Research Communications*, *393*(1), 131–136.

Wang, W. (2007). Emergence of a DNA-damage response network consisting of Fanconi anaemia and BRCA proteins. *Nature Reviews Genetics*, *8*(10), 735–748.

Wu, Y., Sommers, J. A., Khan, I., de Winter, J. P., & Brosh, R. M. (2012). Biochemical characterization of Warsaw breakage syndrome helicase. *Journal of Biological Chemistry*, *287*(2), 1007–1021.